European Journal of Neuroscience, Vol. 25, pp. 3276–3286, 2007 doi:10.1111/j.1460-9568.2007.05559.x

Small-world network topology of hippocampal neuronal network is lost, in an *in vitro* glutamate injury model of epilepsy

Kalyan V. Srinivas, Rishabh Jain, Subit Saurav and Sujit K. Sikdar
Molecular Biophysics Unit, Indian Institute of Science, Bangalore-12, India

Keywords: cross-covariance analysis, hippocampal neurons, multielectrode array, network bursts

Abstract

Neuronal network topologies and connectivity patterns were explored in control and glutamate-injured hippocampal neuronal networks, cultured on planar multielectrode arrays. Spontaneous activity was characterized by brief episodes of synchronous firing at many sites in the array (network bursts). During such assembly activity, maximum numbers of neurons are known to interact in the network. After brief glutamate exposure followed by recovery, neuronal networks became hypersynchronous and fired network bursts at higher frequency. Connectivity maps were constructed to understand how neurons communicate during a network burst. These maps were obtained by analysing the spike trains using cross-covariance analysis and graph theory methods. Analysis of degree distribution, which is a measure of direct connections between electrodes in a neuronal network, showed exponential and Gaussian distributions in control and glutamate-injured networks, respectively. Although both the networks showed random features, small-world properties in these networks were different. These results suggest that functional two-dimensional neuronal networks *in vitro* are not scale-free. After brief exposure to glutamate, normal hippocampal neuronal networks became hyperexcitable and fired a larger number of network bursts with altered network topology. The small-world network property was lost and this was accompanied by a change from an exponential to a Gaussian network.

Introduction

Epilepsy is a common neurological disorder associated with seizures that arise from a collection of neurons that show abnormal and hypersynchronous excitability (Steriade, 2003). While some forms of epilepsy are inherited, a considerable number of epilepsy cases have a known cause and are referred to as 'acquired epilepsy', stroke being one of them. A local lesion due to ischemic stroke leads to increased concentrations of extracellular glutamate (Zhang *et al*., 1995), which causes neuronal injury. In a novel *in vitro* system developed by De Lorenzo's laboratory (Sun *et al*., 2001, 2002), cultured hippocampal neurons in culture, when briefly exposed to glutamate, suffered a neuronal injury similar to that caused by stroke with abnormal epileptiform-type recurrent neuronal discharges in networks of surviving neurons (Sun *et al*., 2001, 2002). While changes in membrane ion permeability have been implicated (Sun *et al*., 2004), changes in the functional organization of the network properties are equally relevant in the generation of hypersynchronous activity, in this *in vitro* model as well as other experimental models of epilepsy. In the present study, we have explored the changes in the neuronal network properties during epileptiform activity *in vitro* in planar two-dimensional neuronal networks cultured on a multielectrode array, using the *in vitro* model of stroke-induced epilepsy. The electrical activity of developing neurons in the network can be recorded as spontaneous extracellular field potentials by the electrodes in the multielectrode array (Chiappalone *et al*., 2005; Van Pelt *et al*., 2005; Evtan & Marom, 2006; Wagenaar *et al*., 2006). The spontaneous activity is characterized by random firing of action potentials during the first week of development. Synchronous spontaneous activity, which represents whole-network activity (network bursts), is observed only after 14–15 days *in vitro* (DIV). The frequency of such network bursts increases as the network grows older (Chiappalone *et al*., 2005; Van Pelt *et al*., 2005). In order to investigate the effect of glutamate injury on developing neuronal networks, hippocampal cultures were exposed to glutamate at 11 DIV and allowed to recover for 4 days. Electrical activity was measured from both control and glutamate-injured networks at 15 DIV. This protocol allowed us to monitor and compare changes in network burst dynamics of glutamate-injured and control networks. Such comparisons may be difficult with older cultures due to the high frequency of network bursts in control cultures themselves (Chiappalone *et al*., 2005; Van Pelt *et al*., 2005). The global properties of the neuronal network can be studied by modelling them as graphs, whose vertices (electrodes) represent the dynamic units and the links represent the interactions between them. Analysis of the complex network suggests that the topology of the network architecture is dynamic and changes during the occurrence of each network burst. In the glutamate-injury model of epileptogenesis (stroke-induced epilepsy), neuronal networks were characterized by a significant increase in the connectivity between the dynamic units accompanied by a breakdown of the small-world property of the network, signified by a decrease in clustering coefficient.

Correspondence: Professor Sujit Kumar Sikdar, as above.
E-mail: sks@mbu.iisc.ernet.in

Received 1 Decemer 2006, revised 12 February 2007, accepted 22 March 2007

Materials and methods

Animals

The ethical committee of Indian Institute of Science, Bangalore, approved the animal experiments described in this study. All efforts were made to reduce the number of animals used.

Neuronal cell culture on multielectrode array

The hippocampal neurons were prepared from Wistar rats (killed by decapitation) on postnatal day 2 and cultured using the following method. The hippocampi of rat pups were dissociated by treatment with 20 units/mL of papain in phosphate-buffered saline supplemented with 10 mM glucose at 37 °C for 30 min, and then plated onto poly D-lysine-coated glass cover slips or on a MED probe (Alpha MED Sciences, Japan), which has 64 planar microelectrodes. A small drop (20 μL) of culture medium with cells, at a density of 3.0×10^3 cells/mm^3 (dense culture), was placed at the centre of the array covering all 64 electrodes. The dissociated neurons were cultured for 15 days at 37 °C in 5% CO_2–95% air at saturating humidity. Half of the culture medium was renewed every 3 days. The medium consisted of Neurobasal-A medium (Invitrogen, USA) supplemented with B-27 nutrients (Invitrogen, USA), 0.5 mM glutamine, 100 U/mL penicillin and 100 μg/mL streptomycin. Biochemicals were obtained from Sigma (USA) unless otherwise specified.

Glutamate injury protocol

At 11 DIV, culture medium was replaced with a physiological recording solution (in mM: NaCl, 145; KCl, 2.5; HEPES, 10; glucose, 10; $CaCl_2$, 2; and $MgCl_2$, 1; with glycine, 2 μM; pH 7.3) in control cultures, and epileptogenic glutamate injury was induced by exposing neuronal cultures to the same recording solution supplemented with 20 μM glutamate for 10 min. Both the cultures were allowed to recover for 4 days. This treatment produced neuronal injury, as previously described (Sun *et al*., 2002). All exposures were performed at 37 °C in a 5% CO_2–95% air atmosphere and terminated by three washes with recording solution and the addition of fresh neuronal feed.

Electrophysiology

Intracellular patch-clamp recordings

Whole-cell current-clamp recordings were performed on pyramidal neurons in both conditions at 15 DIV by using methods described by Sun *et al*. (2001, 2002). In brief, cell-culture medium was replaced with the recording solution described above and recordings were obtained in the whole-cell current-clamp configuration by using an EPC8 amplifier (Heka, Germany). Patch microelectrodes of 3–7 MΩ resistance were filled with an internal solution of (in mM) K^+ gluconate, 140; $MgCl_2$, 1; HEPES, 10; ethylene glycol-bis (β-aminoethyl ether)-N, N, N′, N′-tetraacetic acid (EGTA), 1.1; Na2 adenosine triphosphate (Na_2 ATP), 4; Tris–phosphocreatine, 15; pH 7.2; osmolarity 310 mOsm. Data were digitized and stored on the hard disk of a computer for further analysis. Spontaneous recurrent epileptic discharges (SREDs) were defined as bursts of spike firing at a frequency of ≥3 Hz for durations of ≥20 s. Neurons were categorized as 'epileptic' on manifestation of two or more SREDs; otherwise, neurons were categorized as 'nonepileptic.' Neurons were monitored for a recording period of ≥10 min for the expression of SREDs. All the experiments were carried out at room temperature (25 °C).

Extracellular spike recording using the multielectrode array

The spontaneous activity was recorded on the 15th day after the start of the culture. Experiments ($n = 4$ in each condition) were performed on cultured hippocampal neuronal networks from same batch (sister cultures) in both conditions (control and glutamate-injured). The standard external bathing solution contained (in mM) NaCl, 150; KCl, 3; $CaCl_2$, 2; $MgCl_2$, 1; glucose, 10; and HEPES, 10 (pH 7.3). The extracellular spontaneous activity was recorded with the MED64 system (Alpha MED Sciences, Japan) at a 20-kHz sampling rate. The array consisted of 64 planar electrodes, made up of indium–tin oxide and platinum black, each with a size of 50×50 μm, arranged in an 8×8 pattern with interpolar distances of 150 μm (MED-P5155). All the experiments were carried out at room temperature (25 °C).

Filtering raw signals and spike detection procedures

The electrophysiological signals from the electrodes in the multielectrode array were acquired using commercially available software (Conductor software; Alpha MED Sciences, Japan). Each channel was sampled at a frequency of 20 kHz. The raw signals were converted to comma-separated value (CSV) file format; MATLAB was used for further analysis. Low-frequency baseline shifts in the raw signals were removed using a digital high-pass filter (25 Hz). The threshold (± 8–10 μV) was calculated as multiples of the standard deviation (5 SD) of the signal noise and represented as dashed lines both above and below the signal trace (Fig. 3). Amplitudes exceeding the threshold were regarded as spikes and their time stamps from all 64 channels were saved as a sparse matrix. In this study, no attempt was made to discriminate and sort spikes collected from the channels.

Network burst detection: time alignment

Network bursts gives information about the extent to which a neuronal network fires in synchrony and the number of active sites in the network. For network burst detection in our multielectrode recordings, we used the algorithm as reported (Chiappalone *et al*., 2005; Van Pelt *et al*., 2005), which automatically detects the network bursts from spike trains. The detection is based on the property that, during a network burst, both the number of active sites and the firing rates recorded at the active sites are increased, indicated by a peak in the product of number of active sites and total spike count when evaluated in short time bins. A time bin of 25 ms was chosen in our case, and the multielectrode spike trains were scanned for this product function. An arbitrarily chosen threshold value of 9 (for no. of spikes per time bin × no. of active channels) was well able to distinguish network bursts from the low-level firing periods in between (Fig. 4a and b). Following the detection of a network burst the maximal product bin was searched for among the adjacent bins, while the centre time of a burst was calculated as the centre-of-mass time point for the product distribution evaluated within a window of 5 bins left and right of the centre bin. This centre time point is indicated by a mark (↓) on the top of the network burst profile (Fig. 4c).

Cross-covariance method of edge determination

Connectivity between the channels during network bursts was inferred based on the spike timings during the network bursts, where we sought to determine which electrodes were driving the other electrodes. The

true cross-covariance sequence ($\phi_{x,y}$ (μ)) is the cross-correlation of mean-removed sequences, i.e.,

$$\phi_{x,y}(\mu) = E\{(x_{n+m} - \mu_x)(y_n - \mu_y)\}$$

where μ_x and μ_y are the mean values of the two stationary random processes, and $E\{\cdot\}$ is the expected value operator. Cross-covariance (x,y) returns the cross-covariance sequence in a length $2(N - 1)$ vector, where x and y are length N vectors. The cross-covariance function was applied to all 64 channels at once. In simple words, given the time series information associated with the electrodes, does a spike in electrode X at time t affect the probability of electrode Y spiking at a time $t + k$, where k can be positive, negative or zero. We used cross-covariance instead of cross-correlation to determine edge (the lines connecting the vertices of a graph are most commonly known as graph edges, but may also be called 'arcs' or 'lines'; vertices of the graph are electrodes in our case) connectivity, as cross-covariance corrects for mean firing rates in each electrode, effectively measuring how deviations in firing rate from the expected mean in one recording site are correlated with deviations in firing rate from the expected mean in another recording site. To compute the covariance matrix, we first needed to fill 64 vectors (one for each channel) with digital impulses accumulated at each spike time, and the cross-covariance was estimated for time windows of 10 ms. To accommodate spikes arriving at the edges of a 10-ms window, an extra 2 ms time was given. A threshold value of 5 was chosen to determine edge connection after examining several cross-covariance plots, and fixed for the analysis of all the data sets in the control and glutamate-injured cases (Fig. 6). The network graph topologies were sensitive to the selection of the threshold; low threshold resulted in maximal connectivity, high threshold in poor connectivity, and hence the threshold value was fixed so that the connectivity graphs could be compared in the two experimental conditions. As the distribution of connectivity depends on the selection of the threshold, several network bursts in control and glutamate-treated neuronal networks were similarly analysed at 10 different threshold levels from 2 to 6.5 in steps of 0.5. A threshold value of 5 was found to be the best selection and all the connectivity analysis was done using a threshold of 5. The strength of the connectivity between any two electrodes was reflected by the size of the peak in the cross-covariance plot above the threshold (shown on the graph in Fig. 6a). The methods used for the analysis of multielectrode data were adapted from the work of Ulf Knoblich and Ji-Jon Sit (see: http://web.mit.edu/9.29/www/neville_jen/connectivity/MEA2.htm) for characterization of network topology of multielectrode array network after suitable modifications.

Network topology

The three important parameters in understanding the network topology are defined below.

Degree: the degree, k, of a vertex is the number of other vertices to which it is directly connected.

Path length: the path length (l) between any two vertices, for example x and y, is defined as the number of edges included in the shortest path between them. The characteristic path length (L) of graph G is path length (l) averaged over all pairs of vertices.

Clustering coefficient: another important parameter in the context of small-world networks is the clustering coefficient of the graph. The clustering coefficient of vertex i, C(i), is defined as the number of edges among the k_i neighbours of i (= adjacent vertices), divided by the maximal number of such edges, $k_i(k_i - 1)/2$. Thus, C(i), which is in the range 0–1, measures the 'cliquishness' of the neighbourhood of i, i.e. what fraction of the vertices adjacent to i are also adjacent to each other. By extension, the clustering coefficient C, of the graph G, is the average of C(i) over all vertices (Watts & Strogatz, 1998; Shefi *et al*., 2002). Mathematically, the clustering coefficient of an electrode i is written as

$$C(\mathrm{i}) = 2n_i/k_i(k_i - 1)$$

where n is the number of edges between the k_i nearest neighbours of vertex i.

Results

Glutamate injury induced epileptic activity

Brief exposure to glutamate is known to induce epileptic activity in hippocampal neuronal network cultures (Sun *et al*., 2001, 2002). The *in vitro* model of stroke-induced epilepsy was used to induce seizure activity in our cultures. Hippocampal neurons (11 DIV) were exposed to 20 μM glutamate for 10 min. This glutamate exposure is known to produce death in ~ 40% of the neurons and the surviving neurons develop SREDs (Sun *et al*., 2001, 2002). Patch-clamp recordings were performed in current-clamp mode on control (Fig. 1a) and glutamate-injured (Fig. 1b) neurons at 15 DIV. All the glutamate-injured neurons ($n = 4$) on which recordings were performed manifested SREDs, whereas the control neurons ($n = 4$) showed normal spontaneous firing (< 3 Hz). SRED patterns were quite similar to those reported previously (Sun *et al*., 2001, 2002). As the experimental procedures were also similar to those reported earlier, we would assume the cell loss to be ~40%. Moreover, the neuronal loss was reported to be not greatly influenced by neuronal density and endogenous glutamate levels in the culture media (Sun *et al*., 2001, 2002). The resting membrane potential of the neurons was −61 ± 3 mV. SREDs were characterized by paroxysmal depolarizing shifts and high-frequency firing (> 3 Hz).

Synchronized bursts in neuronal networks

We next explored the changes in the neuronal network properties during epileptiform activity *in vitro,* in planar two-dimensional neuronal networks cultured on multielectrode arrays using the *in vitro* model of stroke-induced epilepsy. Hippocampal neurons from neonatal rat were grown on 8 × 8 multielectrode array; after a few days in culture, dissociated neurons reorganized to establish an elaborate and spontaneously active neuronal network. Figure 1c shows a micrograph of a matured hippocampal neuronal network at 12 DIV. After 14–15 DIV these networks become stable and are characterized by spontaneous, synchronous bursts termed differently by various authors as network bursts (Chiappalone *et al*., 2005; Van Pelt *et al*., 2005), network spikes (Evtan & Marom, 2006), population bursts (Wagenaar *et al*., 2006) or synchronized burst events (Volman *et al*., 2005), and here referred to as network bursts. These bursts become more synchronous as the network grows older (21 DIV onwards; Van Pelt *et al*., 2004; Chiappalone *et al*., 2005). Spontaneous electrical activity was recorded from both control and glutamate-injured neuronal networks (sister cultures) at 15 DIV. The advantage of working with 15 DIV networks, unlike older cultures, is that they display fewer synchronized bursts (Van Pelt *et al*., 2004, 2005) and any changes in burst dynamics can be monitored easily in glutamate-injured networks. Recordings performed on cortical networks in culture media are known to exhibit epileptic behaviour (Wagenaar *et al*., 2005).

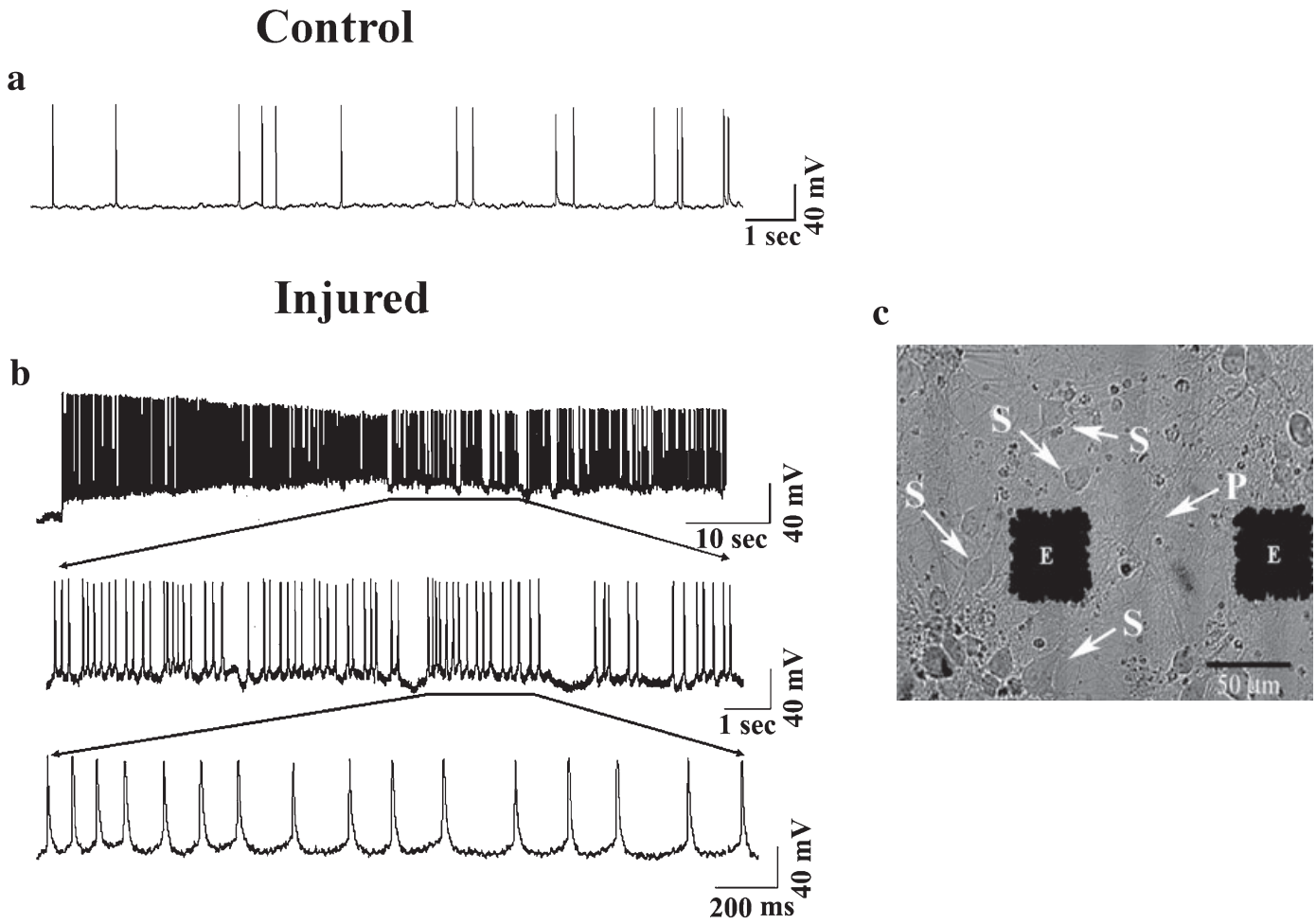

FIG. 1. Glutamate injury induced epileptic activity in individual hippocampal neurons. (a) Spontaneous activity recorded in current-clamp mode from a control hippocampal pyramidal neuron in a network after 15 DIV. (b) Spontaneous activity, indicative of epileptic activity behaviour, recorded from a hippocampal pyramidal neuron 4 days after glutamate injury (20 µM for 10 min). Neurons that survived glutamate injury manifested spontaneous recurrent epileptic discharges (SREDs). Selected portions of the recording are shown on larger time scales in subsequent traces below. (c) Typical hippocampal neuronal network cultured on a multielectrode array probe; 12 DIV. Two recording channels or electrodes (E), embedded in the substrate, with neurons are shown. Typical neuronal somas (S) and processes (P) are indicated with white arrows. Scale bar, 50 µm.

Hence, all the experiments were performed in external solution (see Materials and methods) at 25 °C. Only the first hour of recording was considered for analysis, though the recordings were stable for 2–3 h (survival outside the incubator without the culture medium was the limiting factor). Figures 2a and b show snapshots of 5 s of activity recorded from all 64 channels of a control and glutamate-injured neuronal network. The control networks showed spontaneous activity, which includes random spikes and occasional bursts in a few channels, whereas the glutamate-injured networks showed heightened burst activity in all the channels; this is evident from the raster plots (Fig. 2c and d) of extracted spikes for 100 s of data in the two conditions. The procedure for spike extraction from raw traces of activity is shown in Fig. 3.

Glutamate injury altered network burst dynamics

A network burst represents the period of synchronized activity in the network and, during this transient period, maximum numbers of neurons interact with each other (Van Pelt *et al*., 2005). It has been shown that, like *in vivo* neurons, cortical networks *in vitro* spontaneously synchronize once every 1–20 s, generating assembly activity (network spikes) lasting for 0.1–0.2 s (Evtan & Marom, 2006). Network bursts were separated from the baseline activity using an algorithm described by Van Pelt *et al*. (2005), and similar methods were followed to detect and time-align network bursts in both the experimental conditions (see Materials and methods and Fig. 4a and b). A typical time-aligned network burst is shown in Fig. 4c. Experiments performed on hippocampal networks showed synchronized network bursts of similar durations (Fig. 5a). Glutamate-injured networks also showed network bursts of similar durations (Fig. 5b), but the bursts occurred more frequently. The firing frequency of network bursts in glutamate-injured networks was significantly higher (20.05 ± 2.285/min, mean ± SEM; $n = 4$, $P < 0.0001$) than in control networks (5.4 ± 0.79/min, $n = 4$; Fig. 5c). Moreover, the durations of the network bursts were similar to those of the population bursts (< 200 ms) recorded from acute slice models of epilepsy (Dzhala & Staley, 2003). Time stamps of individual spikes (from all 64 channels) during such time-aligned network burst (for example, see Fig. 5a and b) were collected and stored in a matrix and used to construct the network topology, explained below. Network bursts were detected from segments of 400 s of spontaneous activity in both the experimental conditions.

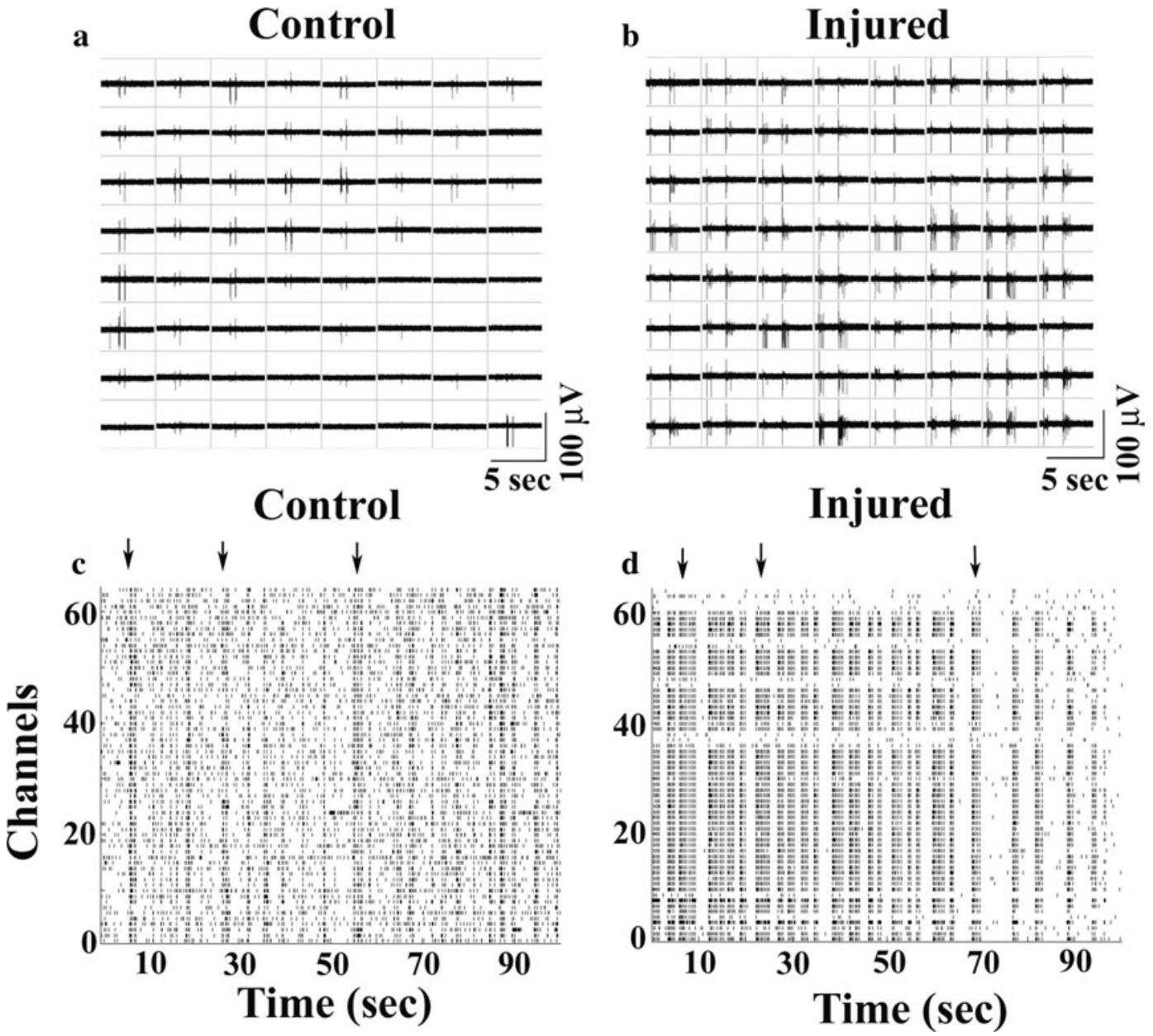

FIG. 2. Glutamate-injured networks showed heightened spontaneous activity compared to control networks at 15 DIV. (a) Snapshot of spontaneous electrical activity recorded from 64 channels (electrodes) in real time from a control hippocampal neuronal network culture. Each window in this and (b) shows 5 s of the recorded signal from a single channel. (b) Snapshot of spontaneous electrical activity recorded from 64 channels from a hippocampal neuronal network culture, 4 days after glutamate injury. (c) Raster plot of spike trains generated from the 64 recording channels of the multielectrode array over 100 s of spontaneous activity from one control network (15 DIV); each row corresponds to a recording site or channel and each small vertical line to a detected spike. The activity consisted of random firing with occasional synchronized activity recorded from most of the channels; this is known as a network burst and is shown with an arrow at the top (↓). (d) Raster plot of spontaneous activity recorded from a sister culture 4 days after glutamate injury. Note the increased spontaneous synchronized activity in the glutamate-injured network compared to control network, on the same day (15 DIV) of recording. Typical network bursts are shown with an arrow at the top (↓).

Analysis of network topology

Network topologies were analysed during the network bursts in control and glutamate-injured neuronal networks. To understand the connectivity pattern, information related to the time series of spike activity recorded from each electrode in the array was analysed using cross-covariance analysis, which corrects for mean spike rates in each electrode, effectively measuring how deviations in firing rate from the expected mean at one recording site are correlated with deviations in firing rate from the expected mean at another recording site. The cross-covariance matrix was computed by filling 64 vectors (one for each electrode) with impulses in defined time bins. An cross-covariance plot of each electrode pair was made next. For 64 electrodes there are $N(N-1)/2$ or 2016 possibilities (N is the number of electrodes). Connections between electrodes were determined by setting an appropriate threshold that was similarly applied to all the data sets. A connection was declared to exist if the cross-covariance value exceeded a certain threshold. For instance, a directed connection between electrodes $1 \rightarrow 9$ was established if the cross-covariance

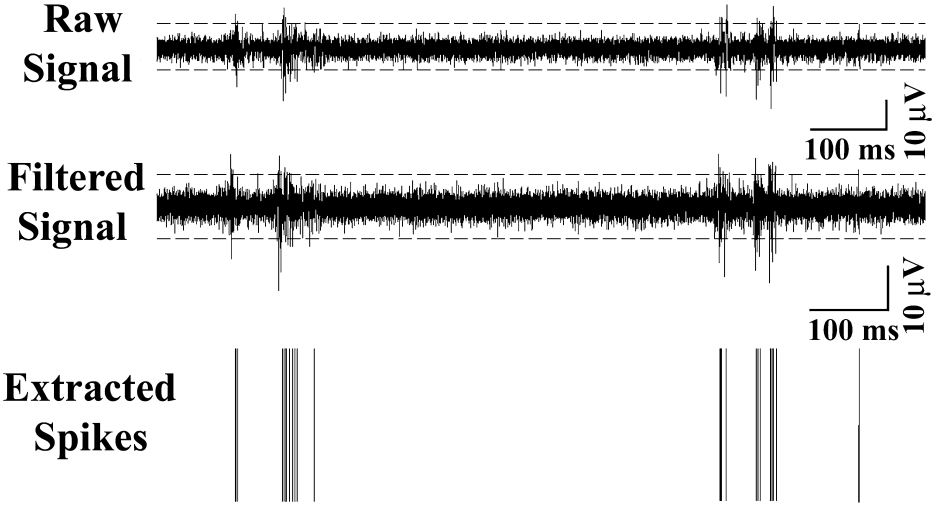

FIG. 3. Filtering of raw electrophysiological data and spike extraction. The top panel shows a raw trace of spontaneous activity from one of the recording electrodes. In the middle panel the filtered signal is shown, the dotted line representing the threshold level of 5 SD. The corresponding extracted spikes are shown in the bottom panel with black lines.

value exceeded a certain threshold at a positive time lag, while a directed connection between 9 → 1 was similarly created if the cross-covariance exceeded the threshold (see Materials and methods) at negative time lag (lag window 60 ms) (Fig. 6a). Part of the connectivity map is shown in Fig. 6b.

A total of 125 network bursts from the two culture conditions were used for the study. Typical network topology of control (Fig. 7a) and glutamate-injured (Fig. 7b) network burst are shown. Glutamate-injured networks showed higher number of direct connections per electrode than did control networks; the average numbers of connections were 33.4 and 7.2, respectively.

Previous studies on cortex of the primate brain (Hilgetag *et al*., 2000; Stephan *et al*., 2000) and nervous system of *C. elegans* (Amaral *et al*., 2000) have shown that these networks demonstrate small-world architectures. Watts and Strogatz introduced the small-world networks concept (Watts *et al*., 1998). A small-world network is one that interpolates between the two extreme cases of, on the one hand, a regular lattice and, on the other, a random graph. It is characterized by a local neighbourhood, which is highly clustered (as in regular lattices), and by a short path length between vertices (as in random networks). To understand whether hippocampal networks exhibit small-world network properties or not, network parameters such as clustering coefficient (C), and characteristic path length (L) and degree (k) or the number of electrodes directly connected to a single electrode were estimated from the connectivity patterns (see Materials and methods). Degree distribution, $P(\mathrm{k})$, gives the probability that an electrode in the network is connected to k other electrodes. Analysis of the way in which the neurons in the electrodes are connected in the control neuronal network cultures suggested that the network is exponential and random (Fig. 7c). The occurrence of highly connected electrodes decreases exponentially. The distribution of connections when plotted on a double logarithmic scale did not fall in a straight line, indicating that the network has no scale. The connectivity distribution was fitted to both a power law, $P(\mathrm{k}) \sim k^{-\lambda}$ ($R^2 = 0.85$) and an exponential, $P(\mathrm{k}) \sim \exp(-\beta k)$ ($R^2 = 0.93$) using regression methods (here $\sim$ means 'follows a function'). An exponential distribution suggests that the hippocampal neuronal network *in vitro* does not have hubs i.e. electrodes that show a very high number of connections. The glutamate-injured neuronal network was described with a Gaussian distribution ($R^2 = 0.9334$), suggesting that it has a random feature, although the average number of connections per electrode (33.4) was significantly higher (Fig. 7d) than that of the control network (7.2; Fig. 7c).

Network topology following glutamate injury

Although the control network topology was exponential and random, it was characterized by high correlation coefficient (C) and characteristic path length (L) values, suggesting that the hippocampal neuronal network is also a small-world network. The clustering coefficient of the network, C, was obtained by averaging C_i over all electrodes of a network (see Materials and methods). The values were 0.43 ± 0.05 and 0.06 ± 0.006 (mean ± SEM) for control and glutamate-injured networks, respectively (Fig. 7e). This corroborates with the values reported for the functional connectivity in the primate cerebral cortex (Stephan *et al*., 2000). The neuronal networks were characterized by relatively small path-length values. Path lengths signify the number of hops required for the impulses to travel from one electrode to another by the shortest path length. The characteristic path length (L), which represents the statistical diameter of the network, was found to be 2.03 ± 0.15 and 1.63 ± 0.14 (mean ± SEM) in control and glutamate-injured networks, respectively (Fig. 7f). The smaller path lengths suggest faster propagation of impulses between the electrodes. However, the glutamate-injured network cultures that are characterized by epileptic discharges did not have small-world properties as a significant decrease in the clustering coefficient was observed, although the characteristic path length did not change (Fig. 7e and f).

Discussion

Neurons that survive the glutamate injury are hyperexcitable and develop SREDs (Sun *et al*., 2001, 2002), but how this property affects the whole neuronal network is not known. We have used a substrate-integrated multielectrode array to measure and characterize the network properties of such glutamate injury-induced epileptogenic networks. Neuronal networks in culture show spontaneous firing activity with short phases of synchronized firing known as network bursts. During such transient periods the whole network is active (Maeda *et al*., 1995; Amioka *et al*., 1996; Jimbo *et al*., 2000; Chiappalone *et al*., 2005; Van Pelt *et al*., 2005). Neuronal networks

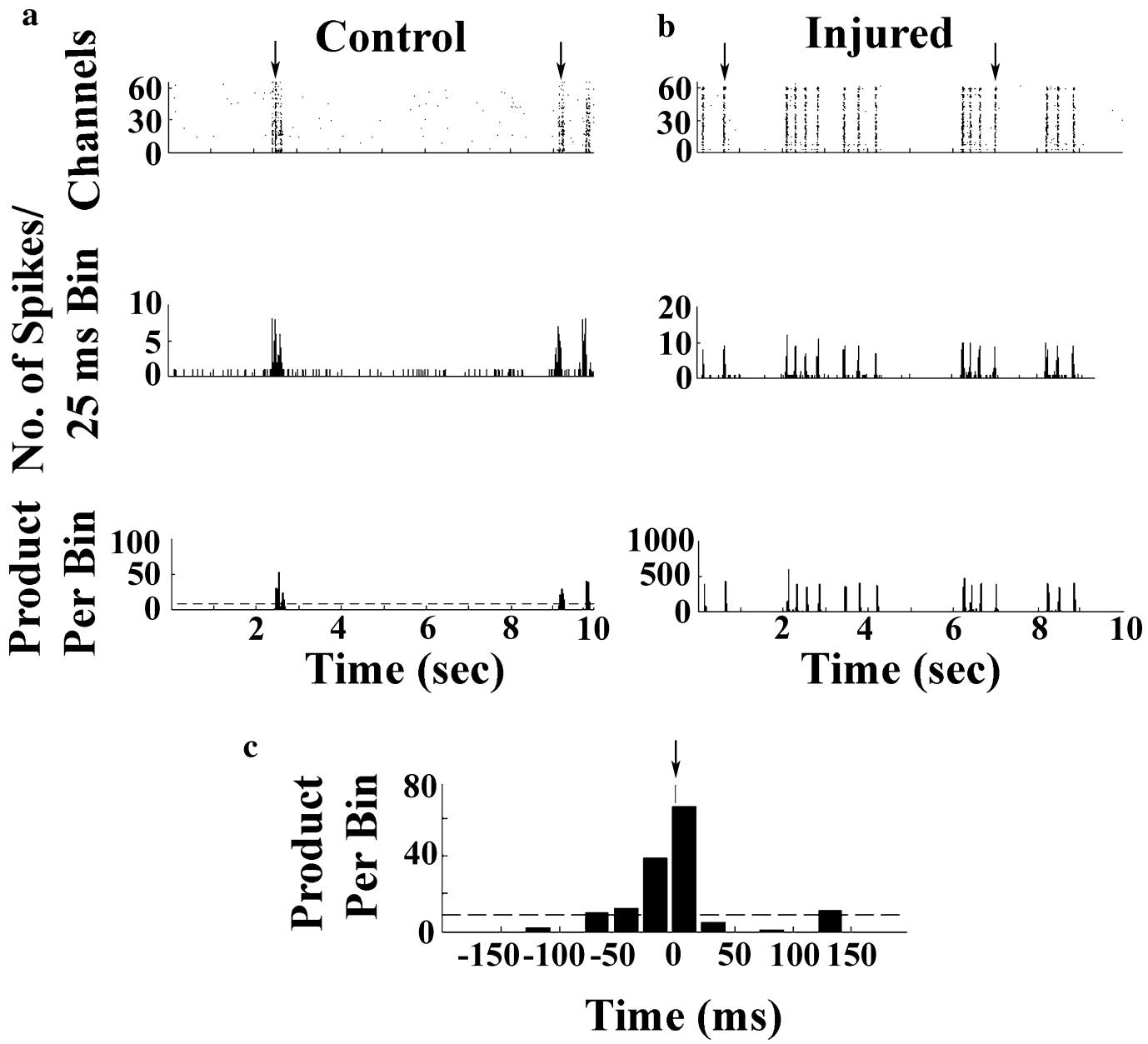

FIG. 4. Network burst detection procedure applied to (a) control and (b) glutamate-injured recordings. In (a) and (b), the top panel shows the raster plot of array-wide activity. The middle panel shows 25-ms binned spike activity, from all 64 electrodes. Product calculation (no. of spikes/bin × no. of active channels) for all the bins and a threshold of 9 (dotted line) to detect the network bursts is shown in the bottom panel. In our experiments, an active channel was defined as a channel presenting two bursts in an acquisition time of 300 s. Examples of detected network burst is indicated with an arrow (↓) at the top of the panel. (c) Procedure for defining network burst duration for analysis of network topology. Example of network burst profiles detected from one of the recording session is presented. The horizontal dotted line represents the threshold of 9. The time bin with maximal product value was taken as the centre bin of the burst and its centre time was considered as the centre-of-mass (COM) point of the product distribution over the bin range of ±5. The COM point is indicated with a small arrow (↓) on the top of the spike count histogram. The value of threshold and the bin range on either side of the COM point were kept constant throughout the analysis.

that survived glutamate injury showed heightened network burst activity compared to control networks. Using network burst detection algorithms, time stamps of individual spikes from each network burst were obtained and connectivity maps were created to understand the propagation of activity between electrodes, which were surrounded by neurons. The cross-covariance method of edge determination revealed that control networks show degree distribution which can be described with exponential decay whereas glutamate-injured networks show Gaussian degree distribution. Interestingly, control networks showed high clustering coefficient (C) and characteristic path length (L) values, which are considered to be small-world properties, whereas glutamate-injured networks showed significantly lower C values although

L remained the same. Small-world architecture of the neuronal network promotes faster signal propagation and synchronization in a network with a small number of connections. Such small-world characteristics have been shown in the nervous system of *C. elegans* (Amaral *et al.*, 2000) and for both structural and functional

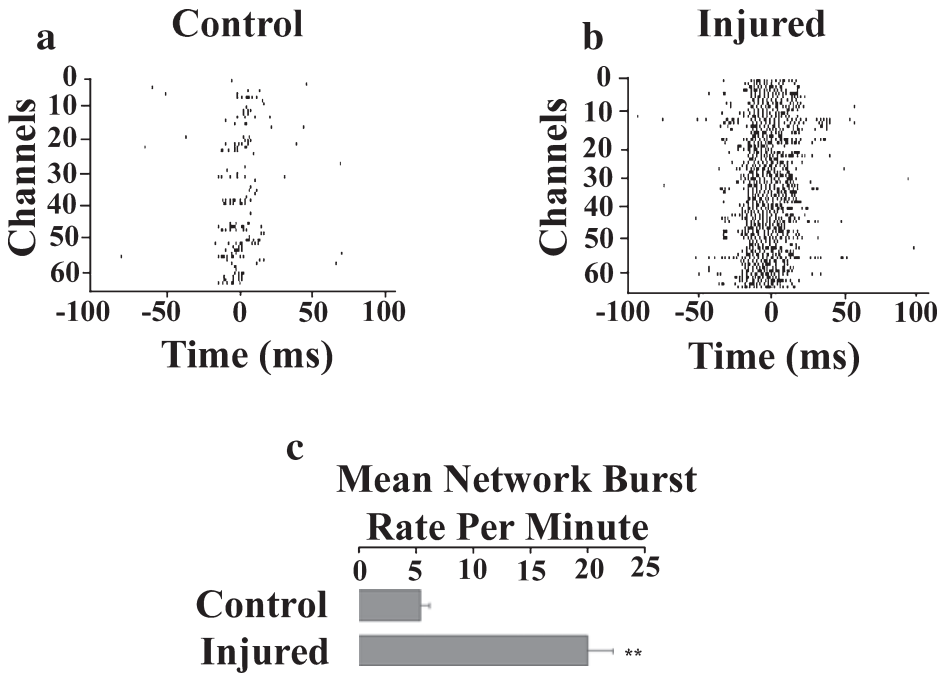

FIG. 5. Glutamate-injured networks showed altered network burst dynamics. (a) A representative network burst recorded from a control network is shown with the activity centred at the centre-of-mass time (0 ms). Typically, a single network burst spread over 100 ms. (b) Raster display of single network burst recorded from a glutamate-injured network; this had a similar duration (100 ms). (c) The frequency of network bursts was different in the two culture conditions. Control networks had a frequency of 5.4 ± 0.79/min whereas glutamate-injured networks had a mean rate of 20.05 ± 2.285/min (mean ± SEM; $n = 4$ in each condition, $^{**}P < 0.0001$, unpaired t-test). Error bar represents SEM.

interactions in the cortex of the primate brain (Hilgetag *et al*., 2000; Stephan *et al*., 2000), besides others. Real-world network (any of various observable phenomena which exhibit network theoretic characteristics, e.g. social networks, computer networks, neural networks, ecological networks and epidemiology) connection distributions are fitted with exponential, power-law, truncated power-law and Gaussian distributions (Amaral *et al*., 2000). There have been suggestions that the neuronal networks are scale-free (Evtan & Marom, 2006). What factors might contribute to the deviation from a scale-free to an exponential network topology as seen in our *in vitro* system? Scale-free networks are growing networks in which new nodes are added preferentially to the more highly connected nodes (Barabasi & Albert, 1999). However, factors such as 'aging', where preferential attachment of new links to the highly connected nodes stops, and 'cost', where the limited capacity of a node to form new links becomes restricted due to physical costs, can change the network topology from a power law to truncated power law (Amaral *et al*., 2000). Mathematical modelling of network growth has suggested that, if the preferential attachment of new nodes to existing nodes of high connectivity is relaxed, the network topologies change to exponential (Krapivsky *et al*., 2000). Other modelling studies indicate that exponential network topology can emerge by rewiring of the existing nodes (Albert & Barabasi, 2000), where the rewiring is not random but is constrained by preferential attachment. Constraints of 'aging' and 'cost' would apply to the development of neuronal connectivity *in vitro* as well. Axonal growth and synapse formation become limited with time, and the number of connections a neuron can develop will be physically limited by metabolic costs related to development and maintenance of connections (Cline, 2003; Laughlin & Sejnowski, 2003). Therefore, it is not surprising that the neuronal network is not scale-free, but exponential. A scale-free topology signifies the existence of hubs, or super-connected neurons. Although scale-free networks are more robust to random damage of nodes, specific damage to the hubs can be lethal. However, super-connected neurons, where a single neuron is connected to many other neurons, have not been reported in the literature so far, although the inability to discover such neurons might be biased by the way connectivity in the brain is established using anterograde or retrograde staining techniques (Humphries *et al*., 2006).

The glutamate-injured neuronal network was described with a Gaussian distribution, suggesting that it had a random feature, although the average number of connections per electrode (33.4) was significantly higher than in the control network (7.2). However, the glutamate-injured network cultures that are characterized by epileptic discharges did not have small-world properties, as a significant decrease in the clustering coefficient was observed although the characteristic path length did not change. This seems to follow the predictions from the model reported by Netoff *et al*. (2004), in which the bursting behaviour associated with epileptic discharges corresponded with a drop in the clustering coefficient, which signaled the transition from a small-world to a random graph. The other important factors that lead to bursting associated with epileptic discharges relate to having a larger number of connections as well as an increase in synaptic strength (Netoff *et al*., 2004). A significant increase in the average number of connections per electrode was observed in the glutamate-injured neuronal network cultures, and changes in synaptic strength associated with epileptiform activity have been reported earlier in the hippocampus (Abegg *et al*., 2004). The changes that are observed with the development of epileptogenesis in the glutamate injury model may also be applicable to the continuous seizure (status epilepticus) injury induced acquired epilepsy model (Sombati & DeLorenzo, 1995; DeLorenzo *et al*., 1998) However, further experiments need to be performed to substantiate this.

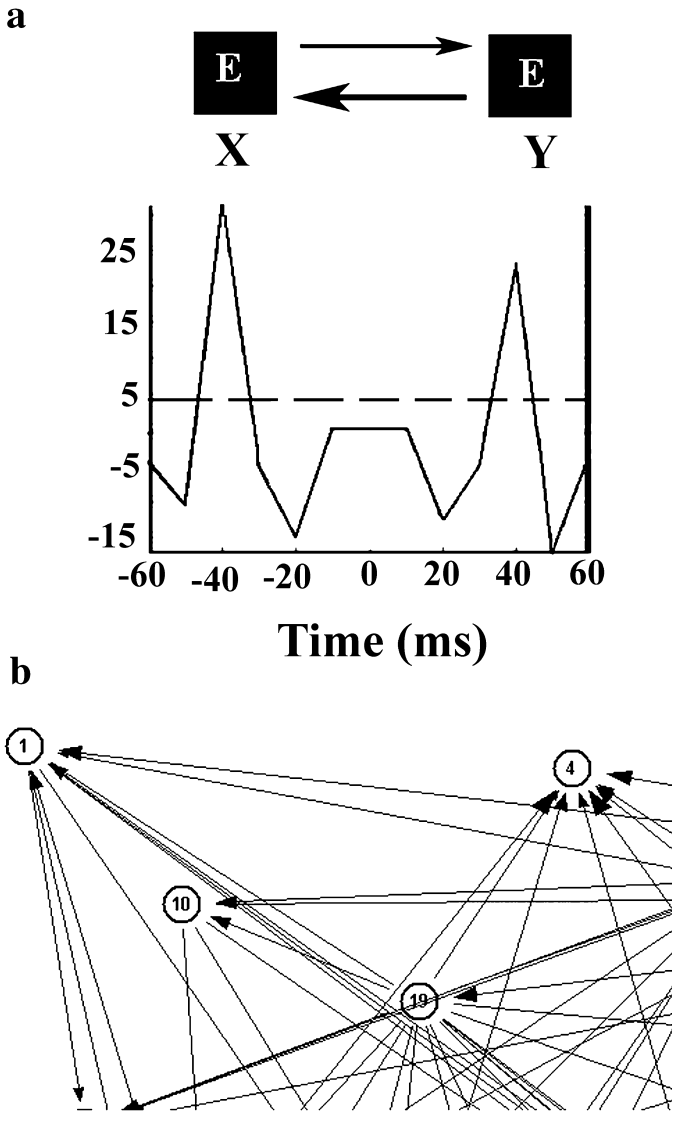

FIG. 6. Cross-covariance method of edge determination. (a) A typical cross-covariance plot, generated between a pair of electrodes, is shown. X and Y are examples of two planar electrodes (black squares with E in the centre). For example, for cross-covariance (X,Y), if the plot exceeded the threshold at a positive time lag then a directed edge X $\rightarrow$ Y was created. If the plot exceeded the threshold at a negative time lag then a directed edge Y $\rightarrow$ X was created. If the plot did not exceed the threshold then no directed edge was generated. The size of the arrow between the channels reflects the size of the peak above the threshold in the cross-covariance plot, with the larger size of the arrow being largest and the smaller size being smallest. For example, note that the size of the arrow directed Y $\rightarrow$ X is larger than that of X $\rightarrow$ Y; this reflects the peak values of the cross-covariance plot. An arbitrarily chosen threshold value of 5 is represented with a dashed black horizontal line. A lag window (x-axis) of -60 to $+60$ ms was chosen for the analysis. The values of threshold and lag window were kept constant throughout the analysis. (b) A part of the edge connectivity graph is shown, where channels 1, 10 and 19 and the connections are seen.

Results of analysis of our experimental data suggest that an increase in connectivity might be one of the mitigating factors that transform a normal neuronal network activity to one with epileptic features. Following glutamate injury the number of electrodes showing activity increased, as shown in Figs 2 and 7. The estimated neuronal loss is $\sim$40%, based on earlier studies (Sun *et al.*, 2001, 2002). Neuronal loss may, however, be accompanied by increase in neuronal sprouting and activity. Analysis of electrode connectivity suggests that there are more connections per electrode (and neuron). The synaptic homeostasis hypothesis has not been explored in the case of neuronal loss situations. It is likely that, in the case of neuronal loss or epileptic conditions, the set point of the synaptic homeostasis mechanism is at a higher level and, to achieve this higher set point, the neuronal network is reconfigured to increase the connections. There appears to be a compensatory response in the neuronal network, whereby the loss of neurons is compensated for by increased connectivity between the existing neurons, although this needs to be substantiated with detailed morphological analysis which is beyond the scope of the current work.

In the case of epileptogenesis, changes in the calcium homeostasis mechanisms appear to play a more important role. Entry of calcium is required to induce the long-term development of the epileptiform discharges in the glutamate-injury model of epileptogenesis (Sun *et al.*, 2002, 2004). The calcium [Ca^{2+}] hypothesis of epileptogenesis proposes that major alterations in calcium homeostasis underlie the maintenance of the epileptic condition. Calcium overload and irreversible loss of calcium homeostasis is known to cause excitotoxic neuronal death (Limbrick *et al.*, 1995). Long-lasting alterations in normal calcium handling, below threshold for excitotoxic cascade activation, may be one of the reasons for the expression of spontaneous recurrent seizures (DeLorenzo *et al.*, 2005). It has now been established in multiple models of acquired epilepsy that the epileptic phenotype is associated with elevated $[Ca^{2+}]_i$ and altered Ca^{2+} homeostatic mechanisms in neurons in the hippocampus and possibly in other brain areas. As Ca^{2+} is such a major second-messenger system, affecting many aspects of neuronal function, it can be assumed that the underlying change in $[Ca^{2+}]_i$ plays a major role in altering neuronal activity (DeLorenzo *et al.*, 2005). The development of epilepsy leads to many changes in the hippocampus, including changes in GABA receptor function (Coulter, 2001), neuronal reorganization (Sanabria *et al.*, 2002), initiation of mossy fibre sprouting (Ben-Ari, 2001; Nadler, 2003), changes in the expression of BDNF (Scharfman *et al.*, 1999; Binder *et al.*, 2001; Scharfman, 2002b), the onset of neurogenesis (Parent *et al.*, 1997; 2002) and other cellular and functional changes (Scharfman, 1992; 1995). Based on the calcium hypothesis and the previous studies on the dependence of epileptogenesis on elevated calcium during the injury phase it is almost certain that these network properties are calcium-dependent. Understanding the molecular basis for these long-term alterations and the possible homeostatic mechanisms that operate to reverse these changes is an interesting area of further investigation and beyond the scope of present study.

The increased connectivity is defined here in terms of number of connections per electrode rather than neurons *per se*, as the covariance analysis was performed without spike sorting. The number of connections per electrode was about four times higher after glutamate treatment than in control (Fig. 7c and d). The anatomical connectivity patterns, consisting of a set of structural connections through synapses linking neurons cultured on the multielectrode array, are expected to be different in the neuronal networks cultured on different multielectrode array probes, as the neuronal networks were formed from randomly dispersed dissociated neurons cultured on the multielectrode array probe ($n = 4$). However, the functional connectivity topologies were surprisingly similar in that they all followed an exponential distribution. Similarly, the network topologies in the glutamate-injured network cultures were consistently Gaussian ($n = 4$). During the 4 days following glutamate injury, and before the electrical activity was sampled, massive alterations in the anatomical connections might have occurred as described below, resulting in significant increases in connectivity between neurons and alterations in the network topology.

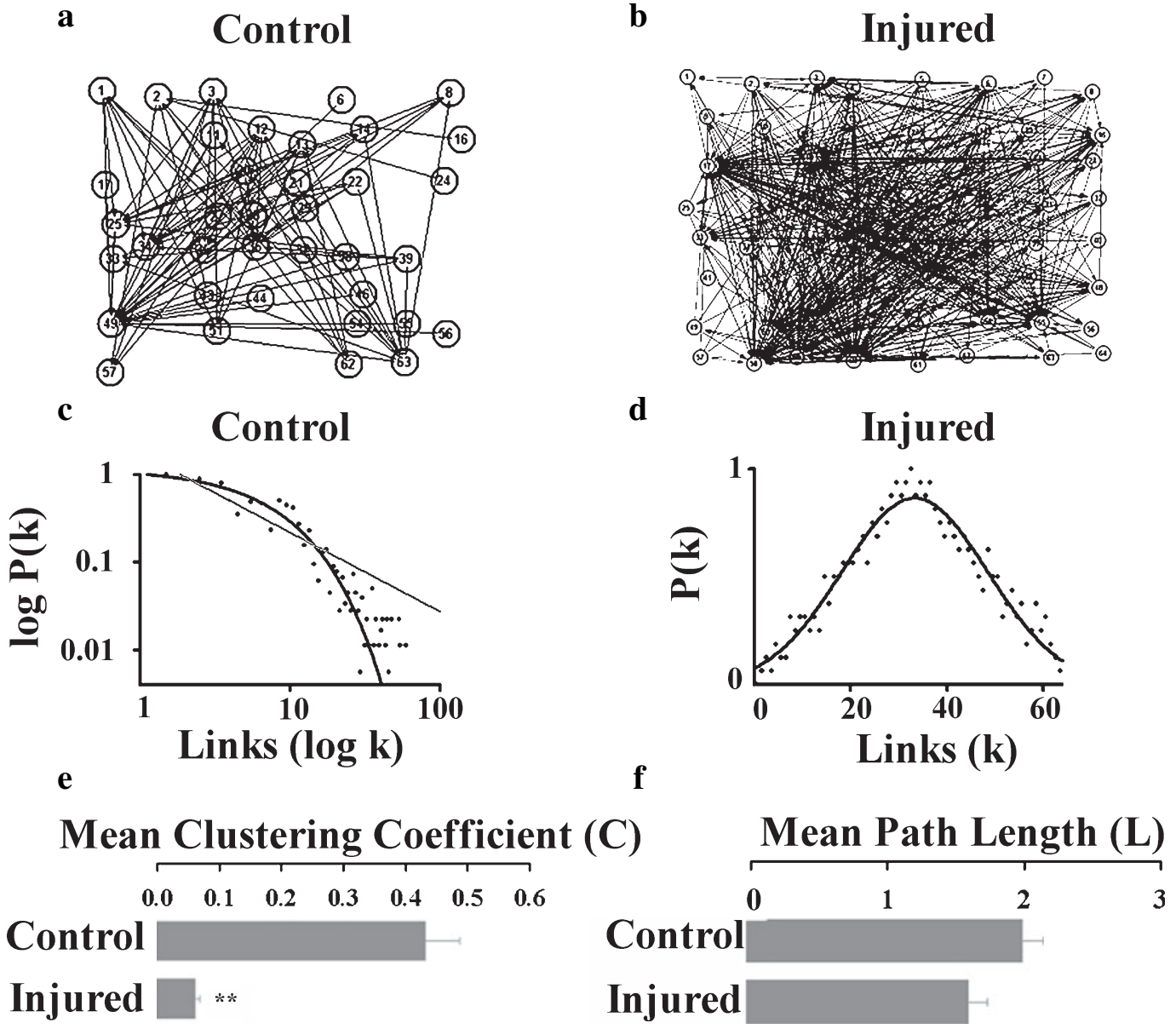

FIG. 7. Glutamate injury affected small-world properties of hippocampal networks *in vitro*. (a and b) Network topology constructed during single network burst in (a) control and (b) glutamate-injured conditions. (c) Degree (links, k) distribution obtained from analysis of 125 network bursts of a control network is shown on a log–log scale. The experimental data (black dots) and the best fits, with both exponential [$P(k) \sim \exp(-\beta k)$, black line; $R^2 = 0.93$] and power law [$P(k) \sim k^{-\lambda}$, grey line; $R^2 = 0.85$], are shown. The mean number (μ) of degrees or links estimated from the exponential fit was 7.2. (d) Similar analysis of a glutamate-injured network is shown. The distribution was Gaussian (R^2 value is 0.9334) on a linear–linear scale with a mean (μ) of 33.4. (e) Bar histograms showing a significant decrease in the mean clustering coefficient (C) in the glutamate-injured condition (0.06 ± 0.006, control; 0.43 ± 0.050, glutamate-injured; $^{**}P < 0.001$, unpaired t-test). (f) The characteristic path length (L) in the two experimental conditions (control, 2.03 ± 0.15; glutamate-injured, 1.63 ± 0.14; mean ± SEM, unpaired t-test) is shown. There is no significant difference. Error bar represents SEM. Similar results were obtained from analysis of network bursts in four different experiments in each condition.

In the course of development, *in vitro*, dissociated neurons become assembled to form functional neuronal networks. The electrical activity of neurons influences the formation of neuronal network structures (Zhang & Poo, 2001). Brief exposure to glutamate in our experiments *in vitro* resulted in a massive change in electrical activity in individual neurons in the neuronal network when recorded 4 days later. Such changes in electrical activity in single neurons would excite the other neurons and bring about structural changes in the neuronal network to alter the network connectivity pattern to a random Gaussian network, with a breakdown of small-world characteristics. In conclusion, we show that neuronal network cultures *in vitro* have a random exponential topology with small-world characteristics that change to random Gaussian topology with a loss of small-world properties following glutamate injury. To our knowledge, these findings represent the first direct documentation of understanding of acquired epilepsy in two-dimensional neuronal networks using multielectrode arrays. Our results also suggest the possibility of similar changes in neuronal network organization during epileptic activity *in vivo*, which remains to be explored.

Acknowledgements

The research was funded by the Department of Biotechnology, Government of India (BT/PR4772/Medical/14/556/2004), with an initial seed grant from the Indian Institute of Science for formation of a Computational Neuroscience Group.

Abbreviations

DIV, days *in vitro*; SRED, spontaneous recurrent epileptic discharge.

References

Abegg, M.H., Savic, N., Ehrengruber, M.U., McKinney, R.A. & Gahwiler, B.H. (2004) Epileptiform activity in rat hippocampus strengthens excitatory synapses. *J. Physiol. (Lond.)*, **554**, 439–448.

Albert, R. & Barabasi, A.L. (2000) Topology of evolving networks: local events and universality. *Phys. Rev. Lett.*, **85**, 5234–5237.

Amaral, L.A., Scala, A., Barthelemy, M. & Stanley, H.E. (2000) Classes of small-world networks. *Proc. Natl Acad. Sci. USA*, **97**, 11149–11152.

Amioka, H., Maeda, E., Jimbo, Y., Robinson, H.P.C. & Kawana, A. (1996) Spontaneous periodic synchronized bursting during formation of mature patterns of connections in cortical cultures. *Neurosci. Lett.*, **206**, 109–112.

Barabasi, A.L. & Albert, R. (1999) Emergence of scaling in random networks. *Science*, **286**, 509–512.

Ben-Ari, Y. (2001) Cell death and synaptic reorganizations produced by seizures. *Epilepsia*, **42** (Suppl. 3), 5–7.

Binder, D.K., Croll, S.D., Gall, C.M. & Scharfman, H.E. (2001) BDNF and epilepsy: too much of a good thing? *Trends Neurosci.*, **24**, 47–53.

Chiappalone, M., Novellinoa, A., Vajda, I., Vato, A., Martinoia, S. & Van Pelt, J. (2005) Burst detection algorithms for the analysis of spatio-temporal patterns in cortical networks of neurons. *Neurocomputing*, **65–66**, 653–662.

Cline, H. (2003) Sperry and Hebb: oil and vinegar? *Trends Neurosci.*, **26**, 655–661.

Coulter, D.A. (2001) Epilepsy-associated plasticity in gamma-aminobutyric acid receptor expression, function, and inhibitory synaptic properties. *Int. Rev. Neurobiol.*, **45**, 237–252.

DeLorenzo, R.J., Pal, S. & Sombati, S. (1998) Prolonged activation of the NMDA receptor–Ca^{2+} transduction pathway causes spontaneous recurrent epileptiform discharges in hippocampal neurons in culture. *Proc. Natl Acad. Sci. USA*, **95**, 14482–14487.

DeLorenzo, R.J., Sun, D.A. & Deshpande, L.S. (2005) Cellular mechanisms underlying acquired epilepsy: The calcium hypothesis of the induction and maintenance of epilepsy. *Pharmacol. Therapeut.*, **105**, 229–266.

Dzhala, V.I. & Staley, K.J. (2003) Transition from interictal to ictal activity in limbic networks *in vitro*. *J. Neurosci.*, **23**, 7873–7880.

Evtan, D. & Marom, S. (2006) Dynamics and effective topology underlying synchronization in networks of cortical neurons. *J. Neurosci.*, **26**, 8465–8476.

Hilgetag, C.C., Burns, G.A., O'Neill, M.A., Scannell, J.W. & Young, M.P. (2000) Anatomical connectivity defines the organization of clusters of cortical areas in the macaque monkey and the cat. *Philos. Trans. R. Soc. Lond. B Biol. Sci.*, **355**, 91–110.

Humphries, M.D., Gurney, K. & Prescott, T.J. (2006) The brainstem reticular formation is a small-world, not scale-free, network. *Proc. R. Soc. Bio.*, **273**, 503–511.

Jimbo, Y., Kawana, A., Parodi, P. & Torre, V. (2000) The dynamics of a neuronal culture of dissociated cortical neurons of neonatal rats. *Biol. Cybern.*, **83**, 1–20.

Krapivsky, P.L., Redner, S. & Leyvraz, F. (2000) Connectivity of growing random networks. *Phys. Rev. Lett.*, **85**, 4629–4632.

Laughlin, S.B. & Sejnowski, T.J. (2003) Communication in neuronal networks. *Science*, **301**, 1870–1874.

Limbrick,D.D., JrChurn, S.B., Sombati, S. & DeLorenzo, R.J. (1995) Inability to restore resting intracellular calcium levels as an early indicator of delayed neuronal cell death. *Brain Res.*, **690**, 145–156.

Maeda, E., Robinson, H.P.C. & Kawana, A. (1995) The mechanisms of generation and propagation of synchronized bursting in developing networks of cortical neurons. *J. Neurosci.*, **15**, 6834–6845.

Nadler, J.V. (2003) The recurrent mossy fiber pathway of the epileptic rain. *Neurochem. Res.*, **28** (11), 1649–1658.

Netoff, T.I., Clewley, R., Arno, S., Keck, T.J. & White, A. (2004) Epilepsy in small-world networks. *J. Neurosci.*, **24**, 8075–8083.

Parent, J. M., Yu, T. W., Leibowitz, R. T., Geschwind, D. H., Sloviter, R. S. & Lowenstein, D. H. (1997) Dentate granule cell neurogenesisis increased by seizures and contributes to aberrant network reorganization in the adult rat hippocampus. *J. Neurosci.*, **15**, 3727–3738.

Parent, J. M., Valentin, V. V. & Lowenstein, D. H. (2002) Prolonged seizures increase proliferating neuroblasts in the adult rat subventricular zone-olfactory bulb pathway. *J. Neurosci.*, **15**, 3174–3188.

Sanabria, E.R., da Silva, A.V., Spreafico, R. & Cavalheiro, E.A. (2002) Damage, reorganization, and abnormal neocortical hyperexcitability in the pilocarpine model of temporal lobe epilepsy. *Epilepsia*, **43** (Suppl. 5), 96–106.

Scharfman, H. E. (1992) Differentiation of rat dentate neurons by morphology and electrophysiology in hippocampal slices: granule cells, spiny hilar cells and aspiny fast-spiking cells. *Epilepsy Res. Suppl.*, **7**, 93–109.

Scharfman, H. E. (1995) Electrophysiological diversity of pyramidal shaped neurons at the granule cell layer/hilus border of the rat dentate gyrus recorded in vitro. *Hippocampus*, **5**, 287–305.

Scharfman, H. (2002b) Does BDNF contributes to temporal lobe epilepsy? *Epilepsy Curr.*, **2**, 92–94.

Scharfman, H.E., Goodman, J.H. & Sollas, A.L. (1999) Actions of brain-derived neurotrophic factor in slices from rats with spontaneous seizures and mossy fiber sprouting in the dentate gyrus. *J. Neurosci.*, **19**, 5619–5631.

Shefi, O., Golding, I., Segev, R., Ben-Jacob, E. & Amir Ayali, A. (2002) Morphological characterization of *in vitro* neuronal networks. *Phys Rev. E*, **66**, 021905.

Sombati, S. & DeLorenzo, R.J. (1995) Recurrent spontaneous seizure activity in hippocampal neuronal networks in culture. *J. Neurophysiol.*, **73**, 1706–1711.

Stephan, K.E., Hilgetag, C.C., Burns, G.A., O'Neill, M.A., Young, M.P. & Kotter, R. (2000) Computational analysis of functional connectivity between areas of primate cerebral cortex. *Philos. Trans. R. Soc. Lond. B Biol. Sci.*, **335**, 111–126.

Steriade, M. (2003) Neuronal substrates of sleep and epilepsy. Cambridge University Press, Cambridge.

Sun, D.A., Sombati, S., Blair, R.E. & DeLorenzo, R.J. (2002) Calcium-dependent epileptogenesis in an *in vitro* model of stroke-induced 'epilepsy'. *Epilepsia*, **43**, 1296–1305.

Sun, D.A., Sombati, S., Blair, R.E. & DeLorenzo, R.J. (2004) Long-lasting alterations in neuronal calcium homeostasis in an *in vitro* model of stroke-induced epilepsy. *Cell Calcium*, **35**, 155–163.

Sun, D.A., Sombati, S. & DeLorenzo, R.J. (2001) Glutamate injury-induced epileptogenesis in hippocampal neurons: an *in vitro* model of stroke-induced 'epilepsy'. *Stroke*, **32**, 2344–2350.

Van Pelt, J., Vajda, I., Wolters, P.S., Corner, M.A. & Ramakers, G.J. (2005) Dynamics and plasticity in developing neuronal networks *in vitro*. *Prog. Brain Res.*, **147**, 173–188.

Van Pelt, J., Wolters, P.S., Corner, M.A., Rutten, W.L.C. & Ramakers, G.J. (2004) Long-term stability and developmental changes in spontaneous network burst firing patterns in dissociated rat cerebral cortex cell cultures on multielectrode arrays. *Neurosci. Lett.*, **361**, 86–89.

Volman, V., Baruchi, I. & Ben-Jacob, E. (2005) Manifestation of function-follow-form in cultured neuronal networks. *Phys. Biol.*, **2**, 98–110.

Wagenaar, D.A., Madhavan, R., Pine, J. & Potter, S.M. (2005) Controlling bursting in cortical cultures with closed-loop multi-electrode stimulation. *J. Neurosci.*, **25**, 680–688.

Wagenaar, D.A., Pine, J. & Potter, S.M. (2006) An extremely rich repertoire of bursting patterns during the development of cortical cultures. *BMC Neurosci.*, **7**, 11.

Watts, D.J. & Strogatz, S.H. (1998) Collective dynamics of 'small-world' networks. *Nature*, **393**, 440–442.

Zhang, J., Benveniste, H., Klitzman, B. & Piantadosi, C.A. (1995) Nitric oxide synthase inhibition and extracellular glutamate concentration after cerebral ischemia/reperfusion. *Stroke*, **26**, 298–304.

Zhang, L.I. & Poo, M.M. (2001) Electrical activity and development of neural circuits. *Nat. Neurosci.*, **4**, 1207–1214.